INNSPUB

Journal of Biodiversity and Environmental Sciences (JBES)
ISSN: 2220-6663 (Print) 2222-3045 (Online)
Vol. 24, No. 2, p. 108-122, 2024
http://www.innspub.net

RESEARCH PAPER OPEN ACCESS

Synthesis and characterization of jackfruit waste based on chitosan nanocomposite for antimicrobial activity and dye absorption photodegradation studies

S. Amutha[1], R. Venkateshwari[1], E. Pushpalakshmi[1], E. Amutha[1], S. Rajaduraipandian[2], M. Vanaja[1], G. Annadurai[*1]

[1]*Sri Paramakalyani Centre of Excellence in Environmental Sciences, Manonmaniam Sundaranar University, Alwarkurichi, India*

[2]*Sri Paramakalyani College, Manonmaniam Sundaranar University, Alwarkurichi, India*

Article published on February 18, 2024

Key words: Chitosan, Jackfruit waste, Antibacterial activity, Photodegradation, Equilibrium studies

Abstract

The aquatic life and populations near the contaminated water sources are seriously at risk for health problems when dye pollutants are disposed of in surface water sources. This study investigated the potential of using a jackfruit waste based on chitosan nanocomposite to treat water contaminated by dyes used in the textile industry. Several techniques, including X-ray diffraction, scanning electron microscopy, fluorescence spectroscopy, Ultraviolet-visible spectroscopy, and Fourier transform infrared spectroscopy, were used to characterize jackfruit waste based on chitosan nanocomposite. Using the batch adsorption method, the suggested adsorbent's adsorption capacity was examined. After carefully adjusting the testing parameters, including the adsorbent dose (0.3 g), initial dye concentration (80 mg/L), contact period (24 hours), solution pH (6.4), and temperature (30 °C), the optimum performance was attained. Utilizing a Jackfruit Waste Based on Chitosan Nanocomposite, Rhodamine dye was able to be removed from water with an efficiency of 90.0% utilizing the Langmuir and Freundlich isotherms, respectively. The adsorbent exhibited heterogeneous surfaces, and Rhodamine Dye adsorbed spontaneously via thermodynamics. Investigations were conducted into the antibacterial activity of Jackfruit Waste Based on Chitosan Nanocomposite. Furthermore, the present results reveal that Jackfruit Waste Based on Chitosan Nanocomposite is promising in future for the removal of organic dyes and other contaminants like toxic heavy metals from water and wastewater.

***Corresponding Author:** G. Annadurai ✉ gannadurai@msuniv.ac.in

Introduction

The processing industry of Jackfruit (*Artocarpus heterophyllus lam*) produced a significant amount of waste, which was disposed of as peel, seed, and latex. If these wastes are not properly disposed of, they are known to result in major environmental issues such greenhouse gas emissions, asphyxiation, offensive odors, and water pollution. The most crucial thing is to use the bioactive compounds from these waste materials for their prospective uses as flavoring, colorant, antioxidant, and texturizing agents (Trilokesh and Kiran Babu, 2023; Antunes and Cavaco, 2010; Fonseca *et al.*, 2002). Animal feed can be made from solid waste that is produced during various unit activities, such as coring and peeling, and has a high nutritional value. If fruit wastes can be transformed into such a variety of value-added goods, the fruit processing facility will turn a profit (Bajwa *et al.*, 2016, Ganesh Moorthy *et al.*, 2017, Chomlog *et al.*, 2019). According to recent reports, significant lignocellulosic biomass made from jackfruit waste was biochemically characterized (Chomlog *et al.*, 2019). The jack fruit tree is widely grown in India and is well-known for its edible fruit and seeds. The waste from non-edible jackfruit is usually burned or dumped in landfills. 13,460 acres are under cultivation for jackfruit in India (Ganesh Moorthy *et al.*, 2017). In India, 2700–11800 kg of non-edible garbage are produced annually (Ganesh Moorthy *et al.*, 2017). A key component in supporting the circular economy might be the biorefinery that uses jackfruit waste to produce bioenergy (Bergstron, 2013).

In the present work, synthesis and characterization of Jackfruit waste based on Chitosan Nanocomposite to explore its form, crystallographic structure, and thermal properties. According to a number of studies, leftover jackfruit can be used to create inexpensive, efficient adsorbents that can be used to remove heavy metals and harmful colors from the environment (Abdulmohsen *et al.*, 2022; Abbas, 2013; Domun *et al.*, 2015; Gu *et al.*, 2013). Peel from jackfruit was chosen as a predecessor because of its inherent durability and strength. The activation method may tolerate harsh circumstances for precursors with high mechanical strength, which increases the yield of adsorbent. The goals of the investigation were to produce a green blend of Jackfruit Waste Based on Chitosan Nanocomposite for photodegradation, antimicrobial activity, and dye adsorption, as well as to synthesize based on Chitosan Nanocomposite by green course using Jackfruit Peel product peels. Gram negative bacteria were tested for the antibacterial qualities of the Jackfruit Waste Based on Chitosan Nanocomposite. In particular, the effects of adsorption and physical and chemical alteration of the jackfruit waste based on chitosan nanocomposite at equilibrium were examined for dye uptake. As a result, a color adsorption process based on chitosan nanocomposite made from fruit peels was presented for jackfruit waste.

Materials and methods

Chemicals, reagents, and media

Analytical grade Raw Chitosan, Glacial Acetic Acid, and Rhodamine dye was purchased from Sigma Aldrich Pvt Ltd, India. Bacterial isolates, Gram-positive *Staphylococcus aureus* and *Bacillus subtilis, and Gram-negative Escherichia coli, Enterobacter sp* and *Pseudomonas fluorescens* were procured from standard vendors.

Preparation of jackfruit peel waste powder

Jackfruit Peel waste was acquired from nearby markets and a local fruit Market. After being carefully cleaned three times with tap water to remove any dirt or water-soluble contaminants, they were roughly chopped into small pieces with a knife and then finely processed using a food processor. They were then dried in an oven set to 50°C for 48 hours after being exposed to the sun for a week until they were crisp. After that, they were powdered and given three successive washes in distilled water to get rid of the color and turbidity. Subsequently, the particles were sieved in order to choose a range of mesh sizes for use as adsorbents in this investigation. For later usage, the fine powder was gathered and kept in an airtight container.

Synthesis of chitosan nanocomposite using jackfruit peel waste powder

The following is how chitosan nanocomposite has been created. 95 ml of distilled water were used to dissolve 1 g of the raw chitosan powder. 5 milliliters of acetic acid were added to this mixture. The solution was agitated for 24 h at room temperature. For twenty minutes, the stirring reaction was conducted. After that, 1 g of powdered leftover jackfruit peel powder was added and stirred for 30 minutes. The reaction was conducted in a boiling water bath with a nitrogen environment and a flow rate of 1 ml/min. Following the completion of the reaction, the final product is dried for two hours at 60°C in a hot air oven.

Photocatalytic activity

Under UV light illumination, the photocatalytic activity of Jackfruit Waste Based on Chitosan Nanocomposite was investigated by measuring the amount of rhodamine dye that degraded in an aqueous solution. To make a suspension, 0.1g of the adsorbent and 0.2 L of dye were mixed together in a known quantity. The suspension was shaken to guarantee that the adsorbent was exposed to light in an even manner. The distance between the bulb and the beaker base under UV light was 13 cm. Throughout each experiment, which was conducted every 180 minutes, a 10 mL sample of a liquid was taken every 20 minutes. After the photocatalyst was removed, the dye degradation was monitored using a Shimadzu UV1650 PC spectrometer and centrifugation at 3000 rpm for 20 minutes. The decreasing absorbance was measured at regular intervals between 0 and 180 minutes.

Batch equilibrium studies

In order to obtain the required concentration of Rhodamine dye solution (20-120mg/L) through equilibrium studies for a 100-ml stock of equilibrium, the Rhodamine dye solution was prepared and diluted. 0.1g of Jackfruit Waste Based on Chitosan Nanocomposite was added to each flask, and it was shaken for the 24hrs. Studies on equilibrium were done at different adsorbent doses (1.0, 2.0, 3.0g/L), temperatures (30°C, 45°C, 60°C) and pH levels (5.4, 6.4, 7.4) Following the solutions' centrifugation, the transparent liquid was measured at 590 nm using spectrophotometer. The equilibrium adsorption rate, q_e (mg/g), was calculated by

$$q_e = \frac{C_I - C_F}{m} \times v \qquad (1)$$

Where, C_I and C_F are the liquid-phase concentrations of dye at initial time and equilibrium (mg/L), consecutively; V is the volume of solution (L); and m is the mass of used dry adsorbent (g).

Antibacterial assay

The antibacterial activity of the Jackfruit Waste Based on Chitosan Nanocomposite was tested using the agar well diffusion method. The bacterial strains were cultured in nutritional broth (NB) at 35°C for the entire night. The inocula of *Pseudomonas fluorescens, Bacillus subtilis, Staphylococcus aureus, Enterobacter sp* and *Escherichia coli* were evenly dispersed on the surface of nutrient agar plates. Different doses of the jackfruit waste based on chitosan nanocomposite (25, 50, 75, and 100 g/mL) were applied. The plates were incubated at room temperature for duration of 24 hours. The antibacterial activity was measured by measuring the inhibitory zone that developed around the well. Following three replicates of each measurement, the means and standard error of the means were calculated.

Results and discussion

UV–visible spectroscopy

The UV-visible diffuse reflectance spectra of the nanocomposite fabricated from jackfruit waste are shown in Fig. 1. The collected UV-visible diffuse spectra at room temperature range from 200 to 1100 nm. While Jackfruit Waste Based on Chitosan Nanocomposite has its absorption peak in the range 520 nm, chitosan increases its absorption edge to longer wavelengths in the range 300-900 nm (Aadr *et al.*, 2008).

The selected concentration of Jackfruit Waste Based on Chitosan Nanocomposite dopant in fruit skin

creates oxygen vacancies as a result of the charge compensation effect, which enables the Jackfruit Waste Based on Chitosan Nanocomposite to migrate towards the visible range (Ahamed *et al.*, 2015; Manjusha *et al.*, 2012). The band gap of the concentration of Jackfruit Waste Based on Chitosan Nanocomposite is 2.60 eV, in agreement with previous research. This highlights the fact that significant changes can be seen in the presence of high chitosan concentrations and that the fruit peel host lattice is closely linked to the apparent absorption phenomenon of Jackfruit Waste Based on Chitosan Nanocomposite.

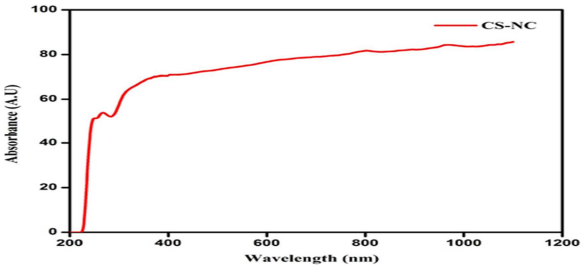

Fig. 1. Absorption spectra of jackfruit waste based on chitosan nanocomposite

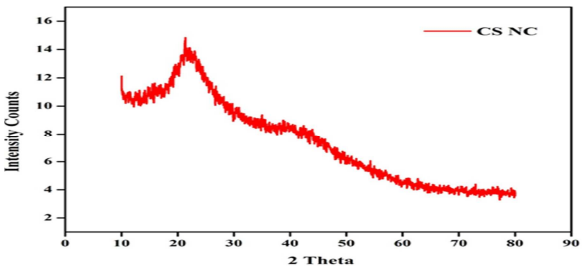

Fig. 2. X-ray diffraction (xrd) analysis of jackfruit waste based on chitosan nanocomposite

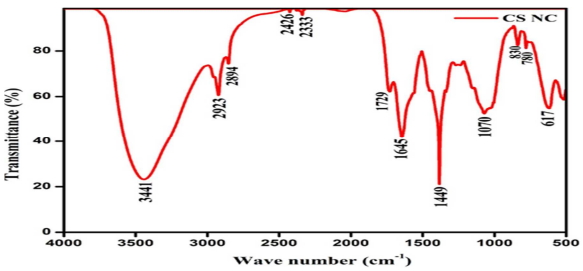

Fig. 3. FTIR spectra of Jackfruit Waste Based on Chitosan Nanocomposite

X-Ray diffraction

The X-ray diffraction patterns of a chitosan and Jackfruit Waste Based on Chitosan Nanocomposite are given in Fig. 2. The XRD pattern's significant crystallinity in the (1 1 1) and (2 0 0) planes was responsible for the distinctive peaks of the Jackfruit Waste Based on Chitosan Nanocomposite (Fig. 2), which were located at 21.84° and 40.6°, respectively (Avinash *et al.*, 2015; Liu *et al.*, 2015; Liu *et al.*, 2016). All of the diffraction peaks provide strong evidence for the cubic anatase structure of the Jackfruit Waste Based on Chitosan Nanocomposite (JCPDS card 00-006-0696). In contrast to the chitosan NPs, the chitosan peaks in the XRD pattern of the Jackfruit Waste Based on Chitosan Nanocomposite were seen to weaken and move right. The peak intensities of the Jackfruit Waste Based on Chitosan Nanocomposite increase with chitosan content, according to the nanocomposite XRD pattern. The stronger hydrogen bonds in the chitosan complex that result from its combination with chitosan could account for these results. Each peak's shape was widened since the chitosan polymer and Jackfruit composite were present.

Fourier transforms infrared spectroscopy

FT-IR spectra of the jackfruit waste based on the chitosan nanocomposite are displayed in Fig. 3. The N–H stretching of hydrogen-bonded amino groups and the C–H stretching vibration of alkyl are represented by the characteristic bands at 3441 to 2923 cm−1, the C–H stretching of CH_2 in fatty acids by the band at 2426 cm−1, and the C≡C terminal alkynes by the band at 2333 cm−1(Avinash *et al.*, 2015; Azhar *et al.*, 2005; Jamroz *et al.*, 2019; oberdorster *et al.*, 2005). The conjugated alkenes with symmetric C=C stretching are responsible for the bands observed at 1729 cm−1. In comparison to the pure Jackfruit Waste based on Chitosan Nanocomposite, the bands shift between 800 and 400 cm−1 because of the presence of C–Br stretch alkyl halides, acetylenic C–H bend alkynes, and C–H bend (mono) aromatics (Camila *et al.*, 2014; Jyotishkumar *et al.*, 2009). The stretching vibration of the C-N stretch aliphatic amines on the surface of the jackfruit waste based on chitosan nanocomposite is responsible for the large peaks that occur at 1070 cm-1 (Zapata *et al.*, 2008).

According to the results of the FTIR study, the fruit peel macromolecules and the C–N stretch aliphatic amines inorganic network were bonded by both covalent and hydrogen bonds in the jackfruit waste based on chitosan nanocomposite, as indicated in (Table 1).

Table 1. Peak and functional group of jackfruit waste based on chitosan nanocomposite

SL	Peak (cm^{-1})	Functional Group
1	3441	N–H stretching with hydrogen bonded amino groups
2	2923	C–H stretching vibration of alkyl
3	2426	C-H stretching of CH_2 in fatty acid
4	2333	C≡C terminal alkynes
5	1729	C=C stretch (conjugated) alkenes
6	1449	C–N stretch aliphatic amines
7	1070	C-H bend (mono) aromatics
8	780	acetylenic C-H bend alkynes
9	617	C–Br stretch alkyl halides

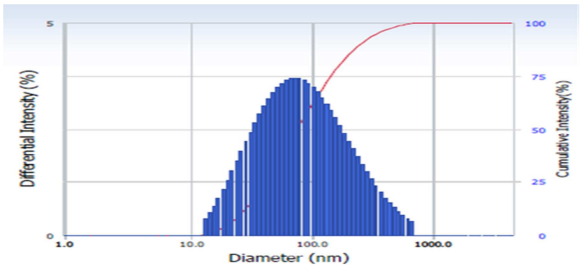

Fig. 4. The particle size and distribution of Jackfruit Waste Based on Chitosan Nanocomposite

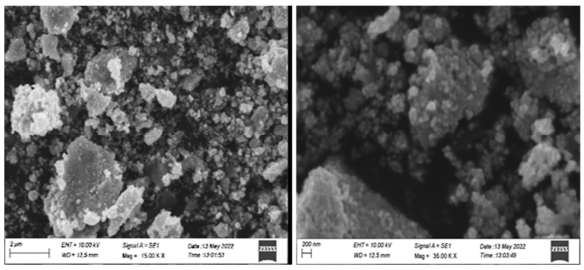

Fig. 5. SEM image of jackfruit waste based on chitosan nanocomposite

Dynamic light scattering

To ascertain the size distribution of the chitosan nanocomposite derived from Jackfruit waste, Dynamic Light Scattering (DLS) was employed. The amount of scattered light that passes through a nanoparticle solution is measured using the DLS technique (Dhand *et al.*, 2016; Domun *et al.*, 2015). The average size was determined using most of the particle sizes present in a sample. The results show that the Jackfruit Waste Based on Chitosan Nanocomposite was synthesized. As seen in Fig. 4, the average size distribution was found to be 74 nm.

Scanning electron microscopy

The size and form of the Jackfruit Waste Based on Chitosan Nanocomposite were assessed by SEM analysis presents the chitosan-based nanocomposite's SEM micrograph of the wasted jackfruit fruit in an easy-to-read manner. The average diameter of the composite particle is around 200 nm, and its particle size is uniform (Egusquiaguirre *et al.*, 2012; Bulut *et al.*, 2006). The backdrop of chitosan and jackfruit waste-based chitosan nanocomposite binding is shown in vivid detail in the Fig. 5.

It was discovered that the chitosan nanocomposite made of Jackfruit waste was widely dispersed and offered a rough surface area for attachment. Jackfruit Waste Based on Chitosan Nanocomposite exhibits uneven nanocomposite clusters with agglomerated and spherical shape, as is seen in Fig. 5.

FL spectroscopy

Fig. 6 displays the fluorescence spectrum of the jackfruit waste-based chitosan nanocomposite. Jackfruit waste based on chitosan nanocomposite was discovered to have a maximum fluorescence peak of 687 nm at the excitation wavelength of the Fluorescence (FL) band, which appears at 591 nm (Elhariry, 2011). These findings show that the concentration and particle size of the chitosan nanocomposite based on jackfruit waste affected both the fluorescence emission band intensity and the absorption band (Faure *et al.*, 2019). The fluorescence spectra of Jackfruit waste based chitosan nanocomposite present at a succession of emission in the domain 300 to 800 nm.

Photocatalytic properties of jackfruit waste based on chitosan nanocomposite

The Rhodamine dye's degradation under UV light was utilized to gauge the photocatalytic activity of Jackfruit Waste Based on Chitosan Nanocomposite.

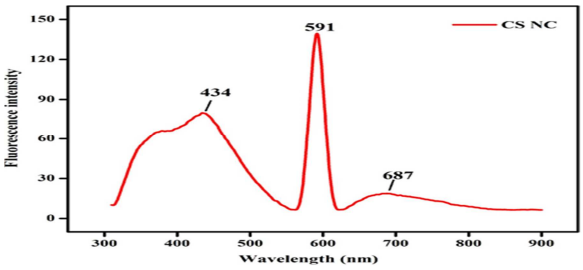

Fig. 6. Fluorescence spectra of jackfruit waste based on chitosan nanocomposite

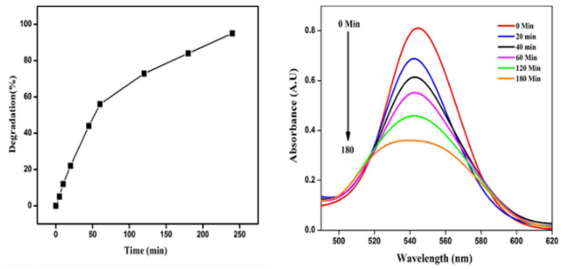

(a) (b)

Fig. 7. (a) Percent degradation of Rhodamine dye with Jackfruit Waste Based on Chitosan Nanocomposite and (b) UV–visible spectra

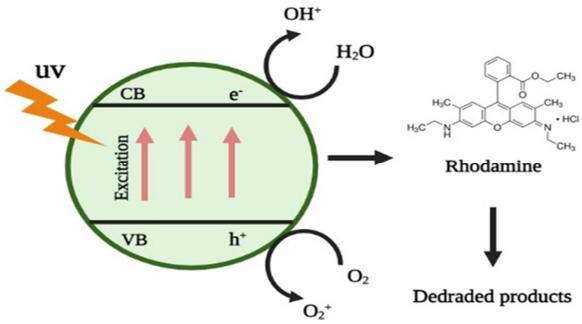

Fig. 8. Reaction Mechanism for the degradation of rhodamine

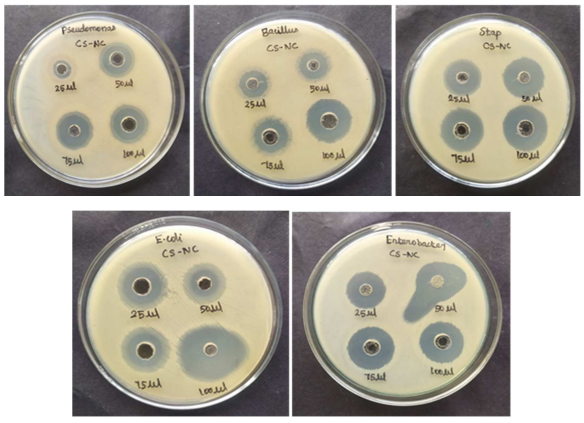

Fig. 9. Zone of inhibition of Jackfruit Waste Based on Chitosan Nanocomposite various bacterial strains

Rhodamine dye is a common industrial pollutant and an important family of synthetic organic dyes used in the textile industry (El Nemr *et al.*, 2009; Ghaffari-Moghaddam *et al.*, 2014). The interaction between the dye molecule and the photocatalyst increased the degradation efficiency (Gu *et al.*, 2013). The Jackfruit Waste Based on Chitosan Nanocomposite that were generated under UV irradiation decolored Rhodamine dye by 94% in around 180 minutes, indicating that silver nanoparticles had completely broken down the dye molecules (Sanchez-Martína *et al.*, 201; Taha *et al.*, 2020). According to Glogowski *et al.* (2006), the increasing removal of the absorption bands of Rhodamine dye indicated that the functional groups that gave the dye its unique color were disintegrating. The time-dependent UV-vis absorption spectra of rhodamine dye in the presence of Jackfruit Waste Based on Chitosan Nanocomposite are displayed in Fig. 7 (a) and 7(b).

Mechanism of photocatalytic degradation of the dye

The breakdown of rhodamine dye is shown in Fig. 8 as a process that is dependent on light. Prior to being exposed to ultraviolet light, the dye is adsorbed on the catalyst's surface (in this case, a Jackfruit Waste Based on Chitosan Nanocomposite - CS NCs). This allows the valence electrons to be excited and migrate from the valence band to the conduction band, lifting a positive hole (h^+) inside the valence band (GuifuZuo *et al.*, 2010; Hameed and El-Khaiary, 2008a; 2008b). Adsorbed water molecules on the surface of the photocatalyst react with positive holes and free electrons to produce ·OH radicals, and free electrons change dissolved oxygen into superoxide anion O_2· radicals. These light-generated radicals degrade the dye molecules into simple molecules like CO_2 and H_2O (Han *et al.*, 2006; 2008; Taha *et al.*, 2020).

$$CS\ NCs + hv \rightarrow e^- + h^+$$

$$H_2O + h^+ \rightarrow OH \cdot + H^+$$

$$O_2 + e^- \rightarrow O_2 \cdot -$$

$$OH + dye \rightarrow degradable\ product$$

$$O_2^- + dye \rightarrow degradable\ product$$

Antibacterial activity

The goal of this work was to assess the synthesized Jackfruit Waste Based on Chitosan Nanocomposite

with its antimicrobial activity and its dependence of that action on the chosen microbial species, namely, *staphylococcus aureus, Pseudomonas* sp*, Bacillus subtilis, Enterobacter and Escherichia* coli. The different species of bacteria shown zone of inhibition in the well diffusion method of antimicrobial activity were investigated (Jayakumar *et al.*, 2010; Kumar *et al.*, 2020). The different patterns of the zone of inhibitions were observed in Fig. 9. Synthesized Jackfruit Waste Based on Chitosan Nanocomposite showed antibacterial activity against both Gram-positive and negative bacteria. Pathogenic bacteria are grown in nutrient broth and 24 hrs culture of these strains were swabbed uniformly onto the individuals plates containing muller hinton agar using sterile cotton swabs (Krishnarao *et al.*, 2012; Jin *et al.*, 2009). About 5 wells were made and the purified Jackfruit Waste Based on Chitosan Nanocomposite at different weight like 25 µl, 50 µl, 75 µl and 100 µl were added into each well on all plates. The plates were incubated for 24 h at 37°C in an incubator. After incubation the different levels of zone formation around the well was measured as shown in (Table 2).

Table 2. Zone of inhibition of Jackfruit Waste Based on Chitosan Nanocomposite against selected bacterial Strains

	Zone of inhibition (mm in diameter)				
Conc.	*Bacillus* subtilis	*E. coli*	*Enterobacter* sp.	*S. aureus*	*P.* fluorescens
25 µl	1.6	1.8	2	2.0	1.2
50 µl	1.9	2	2.4	2.2	1.8
75 µl	2.0	2.4	2.5	2.4	2.0
100 µl	2.2	3.5	2.5	2.6	2.2

S= Staphylococcus, P= Pseudomonas, E= Escherichia, E= Enterobacter

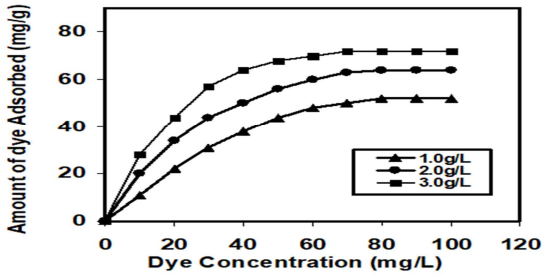

Fig. 10. Effect of Rhodamine dye uptakes at different dosages with dye concentration

Adsorption of rhodamine dye

Effect of adsorbent dosages

As the dosage level was increased and the original dye concentration was lowered, the efficiency of dye removal increased (Azhar *et al.*, 2005). According to Kaur *et al.* (2007), the ideal equilibrium time for different dyes with distinct charcoal adsorbents derived from agricultural leftovers (bagasse, groundnut shells, pea shells, tea leaves, and wheat straw) is between four and five hours. Generally speaking, dye adsorption rose as sorbent dosage increased. Kaur *et al.* (2007) a sorbent dose of 5 (g/L) was applied for acidic dyes, the ratios of dye sorbed had gotten close to their maximum values (Kaur *et al.*, 2007). Hema *et al.* (2007) reported the experimental results of the adsorptions of Rhodamine B (RDB), Malachite green (MG), and Congo red (CR) at different initial concentrations (5, 10, 15, 20, 25, and 30 mg/L) with contact time on activated carbon. As the initial concentration of Rhodamine dye is increased, the % adsorption drops; nevertheless, as the dye concentration increases, the actual amount of dye adsorbed per unit mass of Jackfruit Waste Based on Chitosan Nanocomposite increases (Fig. 10). This indicates that the initial dye concentration has a significant impact on the adsorption (Hema *et al.*, 2007, Shanker and Chinniagounder, 2012) Rhodamine dye solution was used in the studies, initially diluted to 20 to 120 mg/L, and stirred at 30 °C with 0.1 mg/L of jackfruit waste based on chitosan nanocomposite. As illustrated in Fig. 10, adsorption at various dye concentrations began quickly and subsequently decreased progressively as adsorption progressed until equilibrium was attained. El Nemr *et al.* (2009) credit the quick adsorption at the first contact period to the positively charged surface of the Jackfruit Waste Based on Chitosan Nanocomposite. According to Shanker and Chinniagounder (2012), the rhodamine dye solution required a contact period of 24 hours to attain equilibrium. Because of the low ratio of starting dye molecules to surface area at lower concentrations, fractional adsorption becomes independent of starting concentration (Hema *et al.*, 2007). According to Shanker and Chinniagounder (2012), dye molecules must first experience the

boundary layer effect before diffusing from the boundary layer film onto the adsorbent surface and, ultimately, into the adsorbent's porous structure.

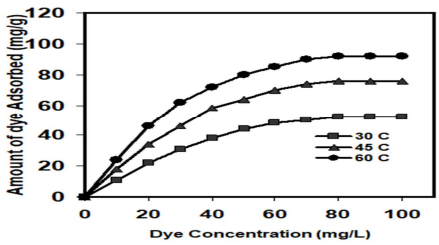

Fig. 11. Effect of Rhodamine dye uptakes at different temperatures with dye concentration

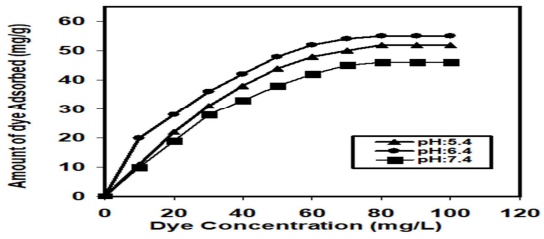

Fig. 12. Effect of Rhodamine dye uptakes at different pH with dye concentration

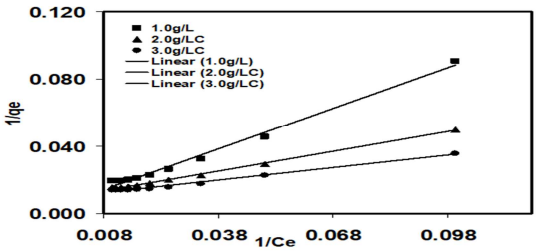

Fig. 13. Langmuir isotherm for the adsorption of Rhodamine dye using Jackfruit Waste Based on Chitosan Nanocomposite at different adsorbent dosages

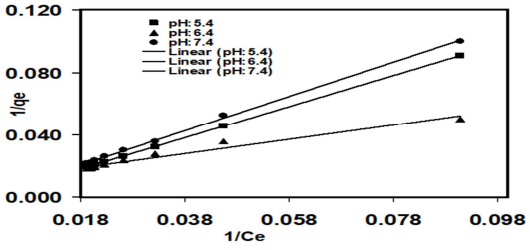

Fig. 14. Langmuir isotherm for the adsorption of Rhodamine dye using Jackfruit Waste Based on Chitosan Nanocomposite at different pH

Fig. 10 shows the impact of an adsorbent Jackfruit Waste based on Chitosan Nanocomposite doses on the elimination of Rhodamine dye from an aqueous solution with a starting concentration of 100 mg/L of Rhodamine dye. According to Pugazhendhi *et al.* (2015), the elimination of Rhodamine dye increased as the adsorbent dose rose. This data can be explained by the fact that an increase in adsorbent dose led to an increase in the number of active sites on the adsorbent surface, which in turn increased the amount of Rhodamine dye removed. The % removal of Rhodamine dye approaches nearly a constant value beyond a certain level (0.3 g for Jackfruit Waste Based on Chitosan Nanocomposite) (Szakiel *et al.*, 2012; Rajan *et al.*, 2015; Poots *et al.*, 1976; Pashaei-Fakhri *et al.*, 2021). The decrease in the gradient in concentration of rhodamine dye molecules could be the cause of this. At optimal conditions, the maximum removal of Rhodamine dye for Jackfruit Waste Based on Chitosan Nanocomposite was found to be 78.0 mg/g (Szakiel *et al.*, 2012; Rajan *et al.*, 2015; Pashaei-Fakhri *et al.*, 2021).

Effect of temperature

Kaur *et al.*, (2007) demonstrated the adsorption of dye at temperature utilizing an environmental Jackfruit Waste Based on Chitosan Nanocomposite. The difference in the adsorbent rate could be caused by the quantity of positive charges present on the sorbent surface, which prevents the negatively charged dye molecule from being rejected and increases adsorption. As temperature increased, so did the dye's adsorption (Fig. 11). For Rhodamine dye at 100 mg/L concentration, the greatest percentage removal of 98.2 mg/g was achieved with an adsorbent dose of 3.0 g/L. The availability of additional surface area for adsorption by the adsorbent was the cause of the rise in dye adsorption with adsorbent dosage. It was discovered that dye adsorption was higher at higher temperatures than it was at lower ones (Lucarelli *et al.*, 2000; Poots *et al.*, 1976; Ho and McKay, 1998a; 1998b; Namasivayam *et al.*, 1998, Namasivayam *et al.*, 2001). The curves show a high tendency for the process to generate monolayers.

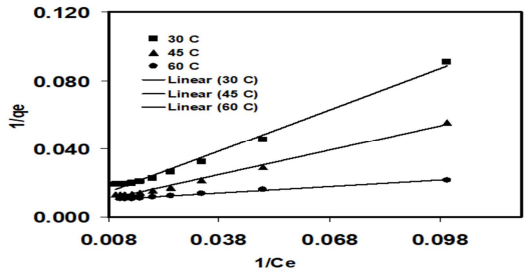

Fig. 15. Langmuir isotherm for the adsorption of Rhodamine dye using Jackfruit Waste Based on Chitosan Nanocomposite at different temperatures

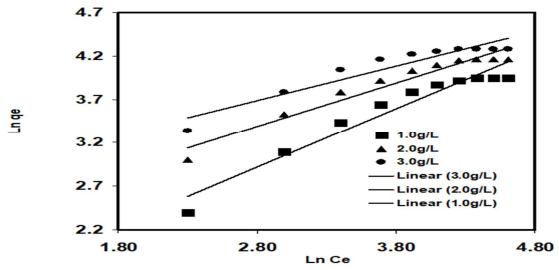

Fig. 16. Freundlich isotherm for the adsorption of Rhodamine dye using Jackfruit Waste Based on Chitosan Nanocomposite at different adsorbent dosages

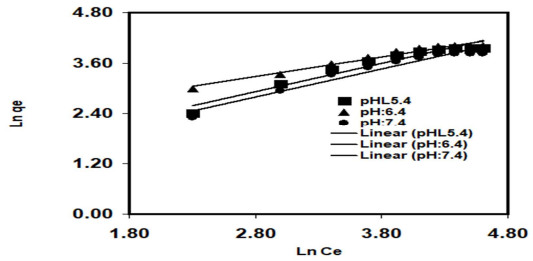

Fig. 17. Freundlich isotherm for the adsorption of Rhodamine dye using Jackfruit Waste Based on Chitosan Nanocomposite at different pH

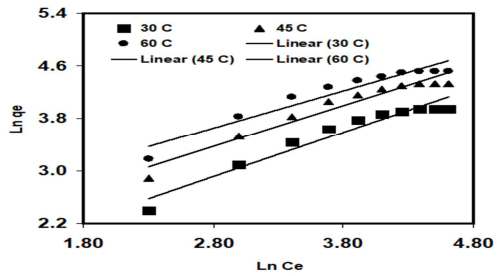

Fig. 18. Freundlich isotherm for the adsorption of dye using Jackfruit Waste Based on Chitosan Nanocomposite at different temperatures

In addition to producing a swelling effect within the internal structure of the nanomaterial, a temperature increase would increase the mobility of the large dye ion and allow the large dye molecule to penetrate further (Namasivayam *et al.*, 2001, Namasivayam and Kavitha, 2002; Ho and McKay, 1999). As a result, the chemical interaction between the functional groups on the adsorbent surface and the adsorbate should be the primary determinant of the adsorption capacity, which should rise as temperature does (Namasivayam *et al.* 2001; Namasivayam and Kavitha, 2002; Ho and McKay, 1999).

Effect of pH

One crucial characteristic that controls the adsorption process is the pH of the solution. This study examined how the pH of the solution affected the utilisation of jackfruit waste to remove rhodamine dye. Based on the study of Chitosan Nanocomposite with varying solution pH, the findings are shown in Fig. 12. As the pH rose from 5.4 to 6.4, there was a rise in the elimination of rhodamine dye. The pH of 6.4 produced the highest percentage of Rhodamine dye removal (Waranusantigul *et al.*, 2003; Yi *et al.*, 2010). The reason for the rise in Rhodamine dye removal as the pH of the solution rises is that at low pH levels, the surface of the adsorbent Jackfruit Waste Based on Chitosan Nanocomposite became more positively charged, which decreased the attraction of Rhodamine dye to the adsorbent's active sites (Mckay *et al.*, 1987). Because the adsorbent surface is more negatively charged at higher pH levels, more Rhodamine dye molecules are drawn to it. The zero point charge of the adsorbent (pHzpc) can be used to describe how pH affects the elimination of rhodamine dye. When the pH of the solution is lower than pHzpc, the adsorbent surface is positive. Because of competition between the ions and positive dye molecules in the aqueous solution, there were fewer dye molecule uptakes under these conditions. Even though the adsorbent surface is negatively charged, the solution pH increase above indicates a modest increase in adsorption-as long as the Rhodamine dye molecules are positively charged (Hameed and Khaiary, 2008).

Table 3. Langmuir and freundlich isotherm constants at different adsorbent dosages, ph and temperatures (rhodamine- jackfruit waste based on chitosan nanocomposite)

Adsorbent Dosage (g/L)	Longmuir Isotherm -model parameters	Freundlich Isotherm -model parameters
1.0	K= 80.63; b= 1.24; R^2= 0.9906	K_F=1.0395; n= 0.96; R^2= 0.9435
2.0	K=35.27; b= 2.58; R^2= 0.9964	K_F=0.9872; n=1.01; R^2= 0.9433
3.0	K= 24.80; b=4.03;R^2= 0.9892	K_F = 2.5704; n= 0.398; R^2= 0.8964
pH	Langmuir Isotherm -model parameters	Freundlich Isotherm -model parameters
5.4	K= 41.55; b= 2.14; R^2= 0.9915	K_F=0.5344; n=0.996; R^2= 0.9435
6.4	K= 80.63; b= 1.24; R^2= 0.9906	K_F=1.0395; n= 0.96; R^2= 0.9435
7.4	K= 70.57; b= 0.93;R^2= 0.9920	K_F= 0.936; n=1.06; R^2= 0.9493
Temperature (°C)	Langmuir Isotherm -model parameters	Freundlich Isotherm -model parameters
30	K= 80.63; b= 1.24; R^2= 0.9435	K_F=1.039; n= 0.96; R^2= 0.9435
40	K=68.29; b= 2.09; R^2= 0.9457	K_F = 0616; n= 0.62; R^2= 0.9457
60	K= 14.11; b= 7.87; R^2= 0.9942	K_F = 0.484; n= 0.531; R^2= 0.9261

The pH of 6.4 was determined to be the ideal value based on the current findings for the upcoming experimental investigations. The initial pH of the solution can have a big impact on how well dyes adsorb. In this instance, the adsorbent's surface (Jackfruit Waste Based on Chitosan Nanocomposite) becomes highly protonated at low pH, or acidic circumstances, which favors the anionic type of adsorption of the aforementioned group of Rhodamine dye. A decrease in adsorption is observed as the pH of the Jackfruit Waste Based on Chitosan Nanocomposite is raised because the surface's degree of protonation gradually decreases (Ofomaja, 2008). Moreover, species of Rhodamine dye and hydroxide ions (OH) compete with one another when pH rises, with the former being the more prevalent species at higher pH levels (Ncibi *et al.*, 2007; Parameswaranpillai *et al.*, 2015). Reduced sorption capacity ultimately results in a decrease in the percentage of Rhodamine dye adsorption. This is because the net positive surface potential of sorbent media decreases, which in turn reduces the electrostatic attraction between the (sorbent) Rhodamine dye species and the (sorbate) adsorbent material surface Jackfruit Waste Based on Chitosan Nanocomposite.

Langmuir and Freundlich isotherm

Adsorption Isotherms the Langmuir and Freundlich (Langmuir, 1916; Freundlich, 1906) models are the two adsorption isotherm models (Eq-2-5) that have been used to characterize the adsorption properties of the adsorbents. The previously stated adsorption isotherm models were examined in their nonlinear version. The Langmuir theory's fundamental premise is that decolorization occurs at particular locations inside the adsorbent. The decolorization experiment data from this study was fitted into an isotherm equation with respect to temperature, pH, and adsorbent doses.

$$q_e = \frac{KbC_e}{(1 + bC_e)} \qquad (2)$$

$$\frac{1}{q_e} = \frac{1}{K} + \frac{1}{KbC_e} \qquad (3)$$

Where C_e is the equilibrium concentration of the Rhodamine dye solution (mg/L), K is the Langmuir constant associated with the affinity of the Rhodamine dye molecule to the adsorbent (L/mg), and q_e is the adsorption capacity at equilibrium (mg/g). Table 3 lists the corresponding coefficient of determination values (R^2) for the adsorption isotherm parameters, which were determined by fitting the adsorption isotherm data to the adsorption isotherm models. The existence of distinct functional groups on the surface and/or varied adsorbent–adsorbate interactions are the causes of the heterogeneity.

A plot of ($1/q_e$ vs $1/C_e$) resulted in a linear graphical relation indicating the applicability of the above model as shown in Fig 13-15. Where q_e is the adsorption capacity at equilibrium (mg/ g), the values are calculated from the slope and intercept of different straight line representing the different adsorbent dosages, pH and temperature (b) energy of adsorption and (k) adsorption capacity and Q_o is represented by (K) as shown in Table 3.

The Langmuir isotherm constant (Q_0) in eqn (3) is a measure of the amount of dye adsorbed, when the monolayer is completed. The Langmuir isotherm and surface can be applied, as shown by the R^2 values, which are almost equal to unity and show a statistically significant linear relationship at the 95% confidence level.

For heterogeneous surface energy systems, the Freundlich isotherm is employed (Ho and McKay 1998; 1998b; Ho and McKay, 1999; McKay *et al.*, 1987; Namasivayam *et al.*, 1998, Namasivayam *et al.*, 2001). The observation revealed that the Freundlich adsorption isotherm model has higher R2 values and lower error values. This suggests that the model provides a more accurate description of the adsorption of Rhodamine dye onto the adsorbents. It was proposed that the adsorbents' heterogeneous adsorption surface. Rhodamine dye and adsorbent affinity was predicted using the separation factor, which was calculated using adsorption isotherm characteristics (Weber and Chakraborty, 1974).

The sorption isotherm is the most convenient form of representing the experimental data at sorbent dosages, pH and temperature as shown in Fig. 16-18.

$$q_e = K_F C_e^{1/n} \quad (4)$$

$$1nq_e = \frac{1nK_F}{\left(\frac{1}{n}\right)1nC_e} \quad (5)$$

The various constants, associated with the isotherm are the intercept, which is roughly an indicator of sorption capacity (k_f) and the slope (1/n) sorption intensity as shown in (Table 3).

Conclusion

In summary, we have successfully prepared an effective adsorption of dyes, photocatalytic and antimicrobial Jackfruit Waste Based on Chitosan Nanocomposite with the help of sol–gel and precipitation method. XRD, UV and FTIR confirmed the Jackfruit Waste Based on Chitosan nanocomposite characteristic featuring nanocrystalline in tetragonal anatase phase. SEM analysis revealed the spherically agglomerated morphology was investigated. The presence of Jackfruit Waste Based on Chitosan Nanocomposite played a vital role in altering physiochemical and antimicrobial activity of Jackfruit Waste Based on Chitosan Nanocomposite. This paper provides a protocol for the synthesis of a new hybrid material which has antimicrobial activity. Jackfruit Waste Based on Chitosan Nanocomposite showed appreciable photocatalytic activity against Rhodamine dye under UV irradiation and the degradation efficiency was estimated to be 94% in 180 min. Overall, According to the FTIR analysis, the Jackfruit Waste Based on Chitosan Nanocomposite has a high concentration of carboxylic, amine, and hydroxyl groups on its surface. These groups promote strong interactions between the adsorbent and the adsorbate, which raises the adsorption capacity and dye removal effectiveness. Anions and cations are present in equal numbers in the wastewater solution, as indicated by the optimal adsorption at pH 6.4. For adsorbent doses more than 0.3 g/L, the adsorption capacity was negligible even though it rise further with adsorbent dose. Due to insufficient adsorption sites, the equilibrium took a bit longer to reach for solution concentrations above 80 mg/L. Nevertheless, the equilibrium was attained within 24 hours of adsorption. The experimental adsorption data was well fitted by a Langmuir and Freundlich isotherm model, indicating that the dye removal procedure utilizing Jackfruit Waste Based on Chitosan Nanocomposite is a good one. This work demonstrates the remarkable adsorption performance of a low-cost, sustainable biowaste-derived Jackfruit Waste Based on Chitosan Nanocomposite towards textile dyes. Furthermore, after undergoing additional acid and basic treatments, approximately 95% of the Jackfruit Waste Based on Chitosan Nanocomposite can be recovered and used again for additional dye adsorption.

Acknowledgements

In order to complete this study S. Amutha (Reg.No.21124012032015) appreciates the Sri Paramakalyani Centre of Excellence in Environmental Science at Manonmaniam Sundaranar University in Alwarkurichi, India

References

Abbas FS. 2013. Dyes removal from wastewater using agricultural waste. Adv. Environ. Biol. **7(6),** 1019–1026.

Abdulmohsen O, Alsaiari S. Shanmugan H, Ahmad B, Essam B, Moustafa RA, Alsulami Iqbal A, Ammar E. 2022. Applications of TiO_2/Jackfruit peel nanocomposites in solar still: Experimental analysis and performance evaluation. Case Studies in Thermal Engineering **38,** 102292.

Aadr Y, Abd El-Wahed MG, Mahmoud MA. 2008. Photocatalytic degradation of methyl red dye by silica nanoparticles. J Hazard Mater **154,** 245–253.

Ahmed MJG, Murtaza A, Mehmood T, Bhatti M. 2015. Green synthesis of silver nanoparticles using leaves extract of Skimmialaureola: Characterization and antibacterial activity. Materials Letters **153,** 10-13.

Antunes, M DC, Cavaco AM. 2010. The use of essential oils for postharvest decay control. A review. Flavour and Fragrance Journal **25(5),** 351–66.

Avik Mukherjee, Vimal Katiyar, Santosh Kumar. 2020. Biopolymer-based nanocomposite films and coatings: recent advances in shelf-life improvement of fruits and vegetables. Indra Bhusan Basumatary **30,** 1912-1935.

Avinash A, Kadam D, Sung L. 2015. Glutaraldehyde cross-linked magnetic chitosan nanocomposites: Reduction precipitation synthesis, characterization, and application for removal of hazardous textile dyes. Bioresource Technology **193,** 563- 567.

Azhar SS, Liew AG, Suhardy D, Hafiz KF, Hatim MDI. 2005. Dye removal from aqueous solution by using adsorption on treated sugarcane bagasse, Am. J. Appl. Sci **2,** 1499-1503.

Bajwa DS, Pourhashem G, Ullah AH, Bajwa SG. 2016. A concise review of current lignin production, applications, products and their environmental impact. Industrial Crops and Products **139,** 111526.

Bergstrom L. 2013. Dispersion and surface functionalization of oxide nanoparticles for transparent photocatalytic and UV-protecting coatings and sunscreens. Sci. Technol. Adv. Mater. **14,** 023001.

Bulut YH. Aydın A. 2006. kinetics and thermodynamics study of methylene blue adsorption on wheat shells, Desalination **194**, 259– 267.

Camila A, de Lima Paulo S, da Silva A. 2014. Chitosan-stabilized silver nanoparticles for voltammetric detection of nitrocompounds. Sensors and Actuators B **196**, 39-45.

Chonlong C, Mohini S, Wensheng Q. 2019. Lignin utilization: A review of lignin depolymerization from various aspects. Renewable and Sustainable Energy Reviews **107,** 232-249.

Dhand V, Soumya L, Bharadwaj S, Chakra S, Bhatt D, Sreedhar B. 2016. Green synthesis of silver nanoparticles using *Coffea arabica* seed extract and its antibacterial activity. Materials Science and Engineering: C **58**, 36-43.

Domun N, Hadavinia H, Zhang T, Sainsbury T, Liaghat GH,Vahid S. 2015. Improving the fracture toughness and the strength of epoxy using nanomaterials- A review of the current status. Nanoscale **7,** 10294–10329.

Egusquiaguirre SP, Igartua M, Hernandez RM, 2012. Nanoparticle delivery systems for cancer therapy: Advances in clinical and preclinical research. ClinTranslOncol **14,** 83–93.

El Nemr A, Abdelwahab O, El- Sikaily A, Khaled A. 2009. Removal of direct blue86 from aqueous solution by new activated carbon developed from orange peel. J. Hazard. Mat **161 (1),** 102-110.

Elhariry HM. 2011. Biofilm formation by Aeromonas hydrophila on green-leafy vegetables: Cabbage and lettuce. Foodborne Pathogens and Disease **8,** 125-131.

Faure B, Salazar-Alvarez G, Ahniyaz, A. Villaluenga I, Berriozabal G, De Miguel YR, Ferdosi E, Bahiraei H, Ghanbari D. 2019. Investigation the photocatalytic activity of $CoFe_2O_4$/ZnO and $CoFe_2O_4$/ZnO/Ag nanocomposites for purification of dye pollutants. Separation and Purification Technology **211,** 35–39.

Fonseca SC, Oliveira F AR, Brecht JK. 2002. Modelling respiration rate of fresh fruits and vegetables for modified atmosphere packages: A review. Journal of Food Engineering **52(2),** 99–119.

Freundlich HMF. 1906. Uber Die Adsorption in Losungen. Zeitschrift fur Physikalische. Chemie **57,** 385.

Ganesh Moorthy J, Prakash Maran S, Ilakya SL, Anitha S, Pooja Sabarima BP. 2017. Ultrasound assisted extraction of pectin from waste *Artocarpus heterophyllus* fruit peel. Ultrasonics Sonochemistry **34,** 525-530.

Glogowski E, Tangirala RT, Russell P, Emrick T. 2006. Functionalization of nanoparticles for dispersion in polymers and assembly in fluids. J. Polym. Sci. A: Polym. Chem **44,** 5076–5086.

Gu Z, Aimetti AA, Wang Q. 2013. Injectable nano-network for glucose-mediated insulin delivery. ACS Nano **7,** 4194-4201.

GuifuZuo, Yizao, WanLeiWang, ChaoLiuFang, HeHonglin Luo. 2010. Synthesis and characterizationof laminated hydroxyapatite/chitosan Nanocomposites. Materials Letters **64(19),** 2126-2128.

Hameed BH, El-Khaiary MI. 2008. Kinetics and equilibrium studies of malachite green adsorption on rice straw-derived charcoal, Journal of Hazardous Materials **153,** 701-708.

Hameed BH, El-Khaiary MI. 2008. Sorption kinetics and isotherm studies of a cationic dye using agricultural waste: Broad bean peels. **154(1-3),** 639-648.

Han R. Ding D, Xu Y, Zou W, Wang Y, Li Y, Zou L. 2008. Use of rice husk for the adsorption of Congo red from aqueous solution in column mode, Bioresour. Technol **99 (8)**, 2938–2946.

Han R, Wang Y, Han P, Shi J, Yang J, Lu Y. 2006. Removal of methylene blue from aqueous solution by chaff in batch mode. J. Hazard. Mater **B137**, 550–557.

Hema M, Arivoli S. 2007. Comparative study on the adsorption kinetics and thermodynamics of dyes onto acid activated low cost carbon. Int. J. Phys. Sci **2**, 10–17.

Ho YS, McKay G. 1998a. Kinetic models for the sorption of dye from aqueous solution by wood, Process Safety Environ Prot **76**, 183-191.

Ho YS, Mckay G. 1998b. Sorption of Dye from aqueous Solution by Peat. Chem Eng J **70**, 115.

Ho YS, McKay G. 1999. A kinetic study of dye sorption by biosorbent waste product pith. Res Conserv Recycling **25**, 171-193.

Jamroz E, Kulawik P, Kopel P. 2019. The effect of nanofillers on the functional properties of biopolymer-based films: A review. Polymers **11 (4),** 675.

Jayakumar R, DeepthyMenon K , anzoora S, Nair V, Tamura H. 2010. Biomedical applications of chitin and chitosan based nanomaterials- A short review. Carbohydrate Polymers **82,** 227-2 32.

Jin T, Sun D, Zhang H. 2009. Antimicrobial efficacy of zinc oxide quantum dots against *Listeria monocytogenes, Salmonella enteritidis* and *Escherichia coli* O157: H7. J. Food Sci **74,** M46-M52.

Jyotishkumar P, Logakis EM, George S, Pionteck J, Häussler L, Haßler R, Pissis P, Thomas S. 2013. Preparation and properties of multiwalled carbon nanotube/epoxy-amine composites, J. Appl. Polym. Sci **127,** 3063–3073.

Kaur S, Walia TPS, Kaur R. 2007. Removal of health hazards causing acidic dyes from aqueous solutions by the process of adsorption. J. Health Allied Sci. **6,** 1-10.

KrishnaRao VK, Ramasubba Reddy S, Yong-IllLee P. 2012. Changdae K. 2012. Synthesis and characterization of chitosan-PEG-Ag nanocomposites for antimicrobial application Carbohydrate Polymers **87(1-4), 920**-925.

Kumar S, Mukherjee A, Dutta. J. 2020. Chitosan based nanocomposite films and coatings: Emerging antimicrobial food packaging alternatives. Trends in Food Science & Technology **97,** 196-209.

Langmuir I. 1916. Constitution and fundamental properties of solids and liquids. I. Solids, J. Am. Chem. Soc. **38 (11),** 2221

Liu H, Kuila Tm Kim, NH, K, BLee JH. 2013. In situ synthesis of the reduced graphene oxide-polyethyleneimine composite and its gas barrier properties. J. Mater. Chem. A **1,** 3739–3746.

Liu L, Yu M, Zhang J, Wang B, Liu W, Tang Y. 2015. Facile fabrication of color-tunable and white light emitting nano-composite films based on layered rare-earth hydroxides. J. Mater. Chem. C **3,** 2326-2333.

Lucarelli L, Nadtochenko V, Kiwi J. 2000. Environmental photochemistry of surface: Adsorption studies and quantitative FT-IR spectroscopy during photo-catalyzed degradation of Azo-dye orange II on TiO_2 surfaces. Langmuir **16,** 1102-1108.

Manjusha M, Suresh kumar, S. Sandhyaran N. 2012. Synthesis and characterization of gold–chitosan nanocomposite and application of resultant nanocomposite in sensorsColloids and Surfaces B: Biointerfaces **93,** 143-147.

Mckay G, Geundi M, Nassar MM.1987. Equilibrium studies during the removal of dyestuffs from aqueous solutions using bagasse pith. Water Res **21,** 1513-1520.

Namasivayam C, Kavitha D. 2002. Removal of Congo red from water by adsorption onto activated carbon prepared from coir pith, an agricultural solid waste. Dyes and Pigments **54,** 47–58.

Namasivayam C, Prabha D, Kumutha M. 1998. Removal of direct red and acid brilliant blue by adsorption on to banana pith. Bioresour Technol **64(1),** 77-79.

Namasivayam C, Radhika R, Subha S. 2001. Uptake of dyes by a promising locally available agricultural solid waste: Coir pith. Waste Manage **38,** 381-387.

Ncibi MC, Mahjoub B, Seffen M. 2007. Kinetic and equilibrium studies of methylene blue biosorption by *Posidonia oceanica* (L.) fibres, J. Hazard. Mater **B139,** 280-285.

Oberdorster G, Maynard A, Donaldson K. 2005. Principles for characterizing the potential human health effects from exposure to nanomaterials: elements of a screening strategy. Part FibreToxicol **2,** 1-35.

Ofomaja AE. 2008. Sorptive removal of Methylene blue from aqueous solution using palm kernel fibre: effect of fibre dose, Biochem. Eng. J **40 (1),** 8–18.

Parameswaranpillai J, Joseph G, Shinu KP, Jose S, Salim NV, Hameed N. 2015. Development of hybrid composites for automotive applications: Effect of addition of SEBS on the morphology, mechanical, viscoelastic, crystallization and thermal degradation properties of PP/PS-x GnP composites. RSC Adv **5,** 25634-25641.

Pashaei-Fakhri S, Peighambardoust SJ, Foroutan R, Arsalani N, Ramavandi B. 2021. Crystal violet dye sorption over acrylamide/graphene oxide bonded sodium alginate nanocomposite hydrogel. Chemosphere **270,** 129419.

Poots VJP, McKay G, Healy JJ.1976. The removal of acid dye from effluent using natural adsorbents. Water Res **10,** 1061-1166.

Pugazhendhi S, Kirubha E, Palanisamy PK, Gopalakrishnan R. 2015. Synthesis and characterization of silver nanoparticles from Alpinia calcarata by green approach and its applications in bactericidal and nonlinear optics. Applied Surface Science **357,** 1801-1808.

Rajan A, Vilas V, Philip D. 2015. Catalytic and antioxidant properties of biogenic silvernanoparticles synthesized using Areca catechu nut. Journal of Molecular Liquids **207,** 231-236.

Sanchez-Martína JM, González-Velascob J, Beltrán-Herediaa J. GrageraCarvajala J, Salguero F. 2010. Novel tannin-based adsorbent in removing cationic dye (Methylene Blue) from aqueous solution, Kinet. Equilib. Stud. J. Hazard. Mater **174,** 9-16.

Shanker M, Chinniagounder T. 2012. Adsorption of reactive dye using low cost adsorbent: cocoa (*Theobroma Cacao*) Shell. World J. Appl. Environ. Chem **1,** 22-29.

Szakiel A, Pączkowski C, Pensec F, Bertsch C. 2012. Fruit cuticular waxes as a source of biologically active triterpenoids. Phytochemistry Reviews. Proceedings of the Phytochemical Society of Europe **11 (2-3),** 263–84.

Taha A, Ben Aissa M, Dana E. 2020. Green Synthesis of an Activated Carbon-Supported Ag and ZnO Nanocomposite for Photocatalytic Degradation and Its Antibacterial Activities. Molecules **25,** 1586.

Trilokesh C, Kiran Babu U. 2023. Kraft lignin from Jackfruit waste as an adsorbent for the selective recovery of biobutanol from the Acetone-Butanol-Ethanol fermentation broth. Biocatalysis and Agricultural Biotechnology **54,** 102966.

Waranusantigul P, Pokethitiyook P, Kruatrachue M, Upatham ES. 2003.Kinetics of basic dye (methylene blue) biosorption by giant duckweed (*Spirodela polyrrhiza*). Environ. Pollut **125,** 385–392.

Weber TW, Chakraborty RK. 1974. Pore and solid diffusion models for fixed bed adsorbents. The Journal of American Institute of Chemical Engineers **20,** 228-238.

Yi L, Yian Z, Aiqin W. 2010. Enhanced adsorption of Methylene Blue from aqueous solution by chitosan-g-poly (acrylic acid)/vermiculite hydrogel Journal of Environmental sciences **22(4),** 486-493

Zapata, P,Raúl Q, Jaime R, Edwin M. 2008. Preparation of nanocomposites by in situ Polymerizations. Journal of the Chilean Chemical Society **10,** 013 1369-1371.